IGM88TC-205-737-G
CNRC 29089

SOLIDIFICATION STRUCTURE OF A STRIP CAST Al-Si-Cu ALLOYS

E. Essadiqi, J. Blain and J. Masounave

Industrial Materials Research Institute
NATIONAL RESEARCH COUNCIL CANADA
75 De Mortagne
Boucherville (Quebec) Canada J4B 6Y4

Presented at the 27th Annual Conference of Metallurgists (CIM)

Montreal, August 28-31 1988

SOLIDIFICATION STRUCTURE OF A STRIP-CAST AL-Si-Cu ALLOYS

E. Essadiqi, J. Blain and J. Masounave

Industrial Materials Research Institute
NATIONAL RESEARCH COUNCIL CANADA
75 De Mortagne
Boucherville (Quebec) Canada J4B 6Y4

ABSTRACT

Microstructures of as-cast 1060 and 380 (Al-9.2% Si-3.3% Cu) aluminum alloys made by a twin-roll caster were determined. A cellular structure was found in 1060. In the case of 380 alloy a dendritic structure of αAl was formed along with the eutectic Al-Si-Al_2Cu in the interdendritique regions. The segregation in the 380 alloy shows that the central zone corresponds to higher microsegregation for the Al, Si, Cu and Fe with also the presence of microporosity. Thermal analysis was conducted on casting in a static horizontal mold and a solidification model has been devised for the calculation of the heat transfer coefficient, which was found to be in the range of 1.6 - 2.0 $kW/m^2 \cdot K$. The secondary dendrite arm spacing, λ, in 380 alloy shows a linear relationship on a logarithmic scale with the distance from the wheel. By using the heat flow model, it was found that λ is related to the local solidification time by the equation $\lambda = 10.10\ t_f^{0.43}$. The value of the heat transfer coefficient for the strip casting of the aluminum alloys is around $9 \cdot KW/m^2 \cdot K$, which is much higher than in the static case.

KEYWORDS

Strip casting, twin roll caster, Al alloys, solidification, segregation, dendrites, modelling, heat transfer, microstructure.

INTRODUCTION

Increased competition in the material producing market has lead to a renewed interest in strip casting technologies. This process can potentially eliminate part of the hot rolling, save energy and offer the possibility of producing new alloys in strips. High cooling rates associated with this process are desirable in metallurgical and production rate terms. In this perspective we have developed a process using a vertical twin roll caster (Masounave, Blain and Essadiqi, 1988). We will focus in this study on the microstructure of two aluminum alloys, the segregation obtained by this process and the heat transfer between the strip and the rolls. Some static experiments were also carried out to analyse the heat flow within the two alloys during solidification.

EXPERIMENTAL PROCEDURES

The twin roll caster shown in Fig. 1 is used to cast a horizontal strip. The twin rolls are made of pure copper coated with graphite with no cooling system. The chemical compositions of the two aluminum alloys cast and the experimental conditions are given in Tables 1 and 2 respectively. The physical properties of the above materials are summarized in Table 3. In this study the process is controlled by the speed of the rolls which is decreased from 15 RPM until the strip exits as a solid.

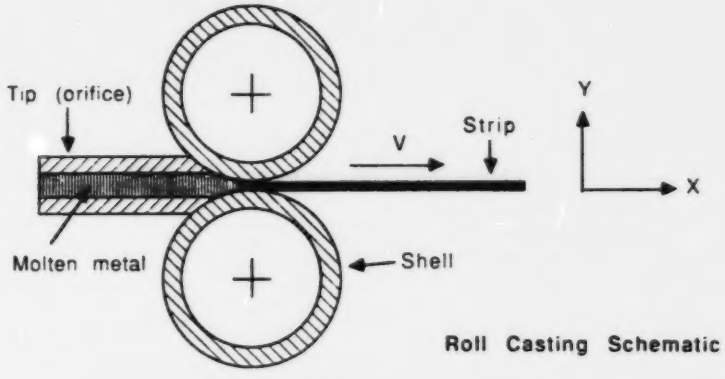

Fig. 1. Twin-roll strip caster (schematic)

150 kg of aluminum alloy was melted in an induction furnace. The melt was poured into a tundish and injected into the twin roll caster through a refractory nozzle. The casting speed was 2 to 14 RPM depending on the contact angle which was set anywhere from 7 to 14 degrees. The cast strip was 2 mm in thickness and 10 cm in width.

Experiments with a static copper mold coated with graphite were also done with the two alloys. The evolution of the specimen temperatures during solidification was monitored by means of Chromel-Alumel thermocouples.

Metallography

After mechanical polishing, the Al 1060 samples were etched with Flick's reagent (Davies and Brook, 1983): HCl: 15 ml; HF: 10 ml; Water: 90 ml. The etching time was 20 to 30 s.

The 380 alloy samples were etched with the following reagent (Gruzel and Kurz, 1987) for about 10 s: $K_3Fe(CN)_6$: 5 g; NaOH: 10 g; H_2O: 60 ml

Table 1 Chemical analysis of the aluminium alloys

Material	Si	Cu	Zn	Fe	Mg
1060	.07	--	0.01	0.18	--
380	9.16	3.25	2.41	0.84	0.05

Table 2 Experimental conditions for the aluminum alloys

Material	Liquid Temperature To	Speed RPM	Contact angle
1060	705	5	7°
380	615	5	7°

Table 3 Physical properties of 380 and 1060 Al alloys (McCall and co-workers, 1979)

Material	1060	380
Density (kg/m^3)	2705	2740
Liquidus T_L (°C)	657	572*
Solidus T_S (°C)	646	550*
Latent heat (kJ/kg)	390	389
Specific heat (J/kg•K)	900	963
Thermal conductivity (W/m•K)	234	96.2

*these values have been determined experimentally.

Segregation analysis

The segregation of Al, Si, Cu, Zn and Fe was investigated by microprobe analysis using a Jeol 35 SEM equiped with a TRACOR WDX system.

EXPERIMENTAL RESULTS

1060 alloy

All the strips obtained had smooth surfaces. Figure 2 shows a typical structure of a transverse section where it can be seen that the surfaces have an undercooled structure (≈ 20 μm) followed by a columnar zone parallel to the flow direction of heat extracted by the wheel. The third zone corresponds to the cellular structure. At the centre of the strip there is a boundary resulting from the intersection of the two solidification fronts. The columnar grains are slightly tilted with respect to the wheel surfaces as has been observed by Morris and Morris (1987); Black and co-workers (1985); Bowman and Antolovich (1986).

380 Alloy

The characteristic structure is shown in Fig. 3. It shows dendrites of aluminum solid solution (white areas) with a eutectic in the interdendritic spaces. Close to the surfaces, when there has been good contact between the strip and the

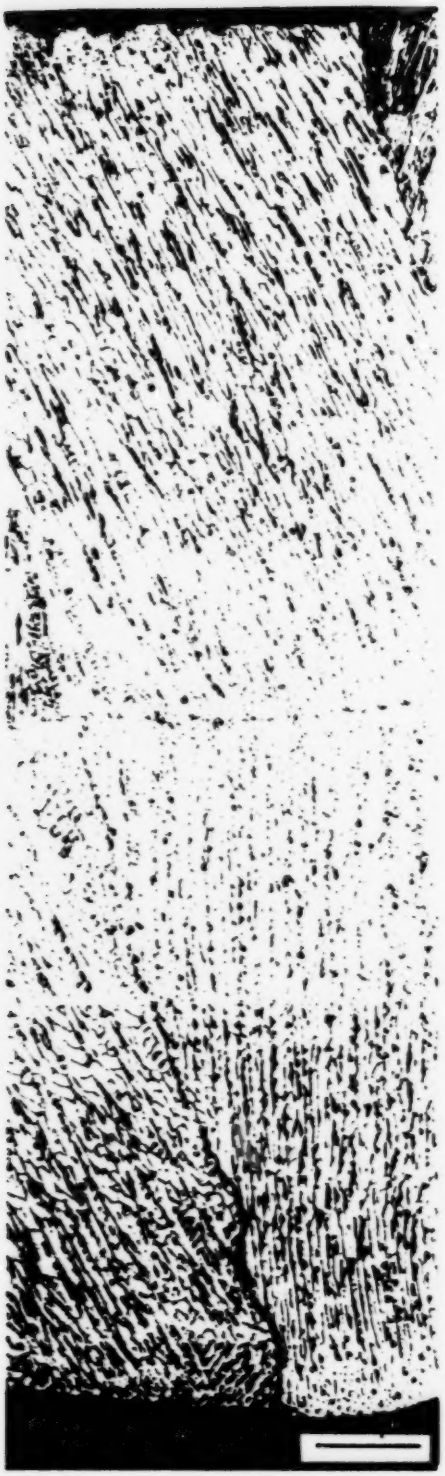

Fig. 2. As-cast structure of 1060 aluminum alloy across the thickness showing columnar cellular structure.

Fig. 3. As-cast structure of 380 aluminum alloy across the thickness showing αAl dendrites (white area) and the eutectic (dark area).

substrate, the primary dendrites are parallel to the heat flow (Fig. 4). The secondary dendrite arm spacing becomes coarser as the distance from the wheel increases (Fig. 5). This phenomenon is related to the cooling rate as is explained later.

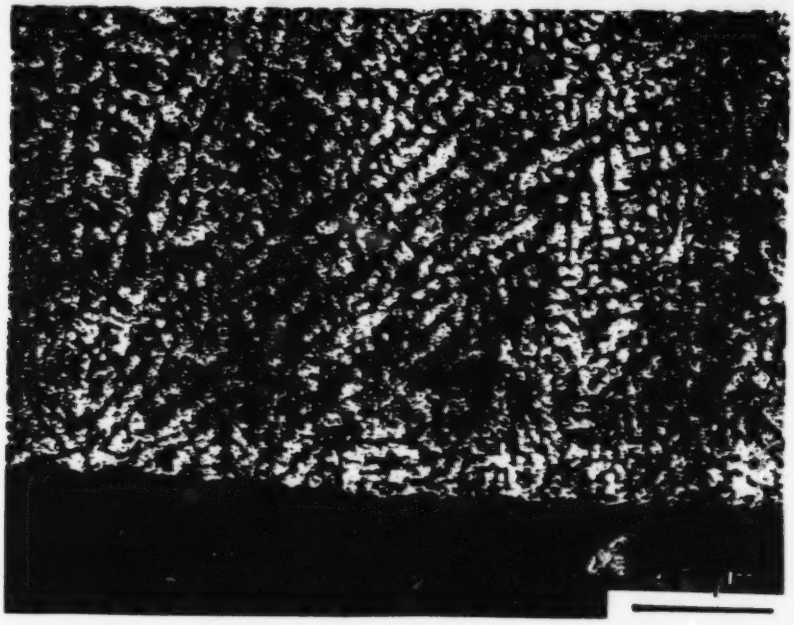

Fig. 4. As-cast structure of 380 aluminum alloy close to the wheel surface.

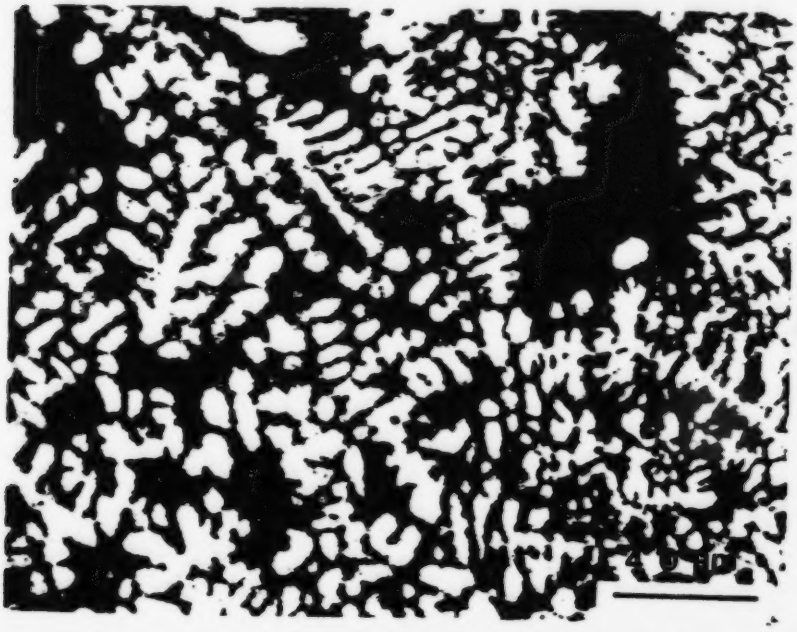

Fig. 5. As-cast structure of 380 aluminum alloy at the centre of the strip

Segregation

The microprobe profile analyses of Al, Si, Cu, Zn and Fe across the strip thickness are illustrated in Fig. 6. It can be seen that the strip composition

did not vary significantly from one surface to the other. However, there is local segregation with formation of the eutectic, Al-Si-Al_2Cu, which consists of Si and the intermetallic compound θ (Al_2Cu) in a matrix of aluminum solid solution. Fig. 7 shows the eutectic structure; the compound Al_2Cu is white and Si is dark. From the profile of all the elements, it can be seen that the central zone corresponds to higher microsegregation. This is due to the lower cooling rate and the classical centre line segregation. The eutectic was analysed by examining the wave lengths of the characteristic X-ray emission lines in scanning electron

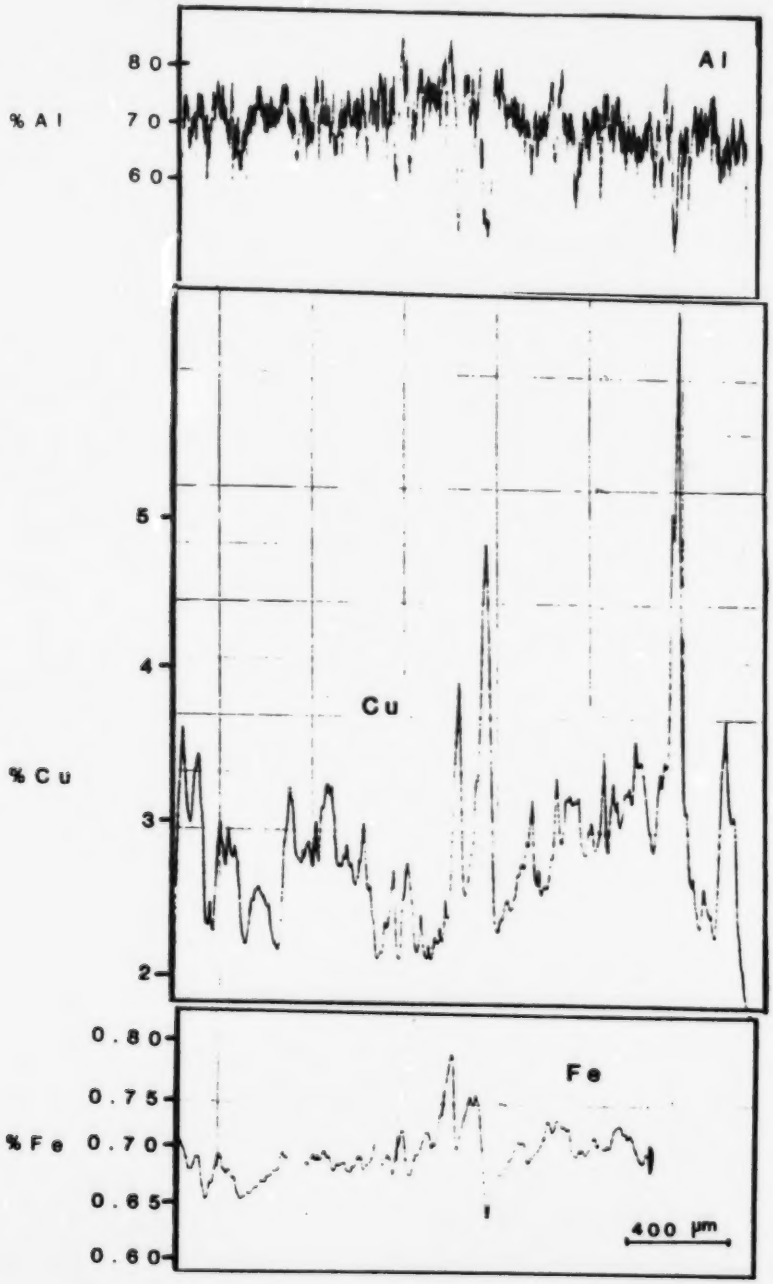

Fig. 6. The distribution of Al, Cu, and Fe across the thickness of the as-cast 380 aluminum alloy.

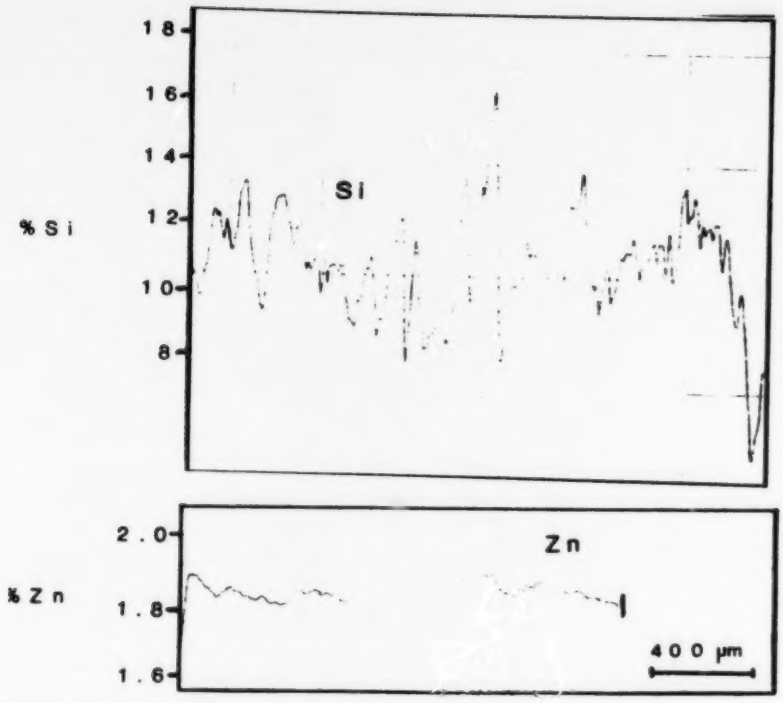

Fig. 6. The distribution of Si ans Zn across the thickness of the as-cast 380 aluminum alloy.

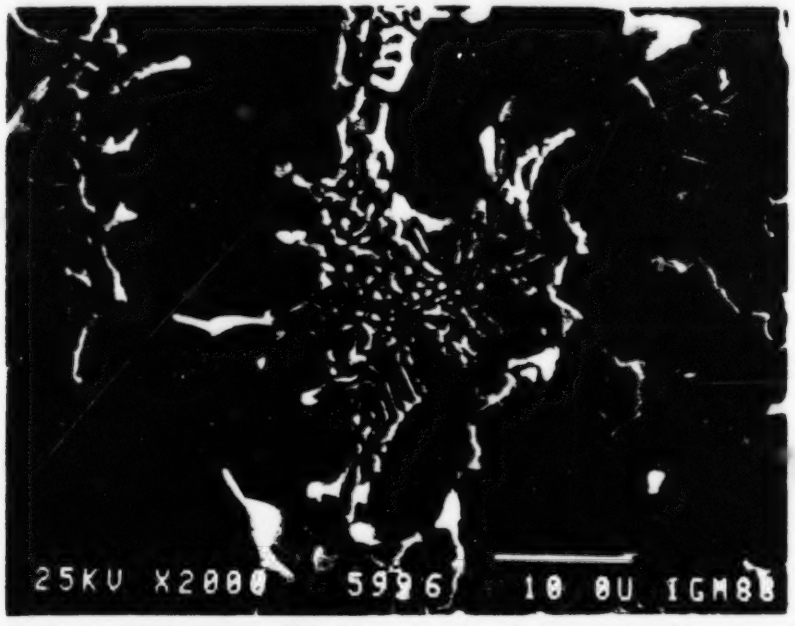

Fig. 7. High magnification SEM micrograph of the eutectic structure in the as-cast 380 aluminum alloys.

microscopy of the Al, Si and Cu. The area analysed is shown in Fig. 8a-d. By reference to the X-ray profiles of Al, Si and Cu. In Fig. 8a the dark phase corresponds to the Al phase, the slightly medium gray to Si and the white to Al_2Cu.

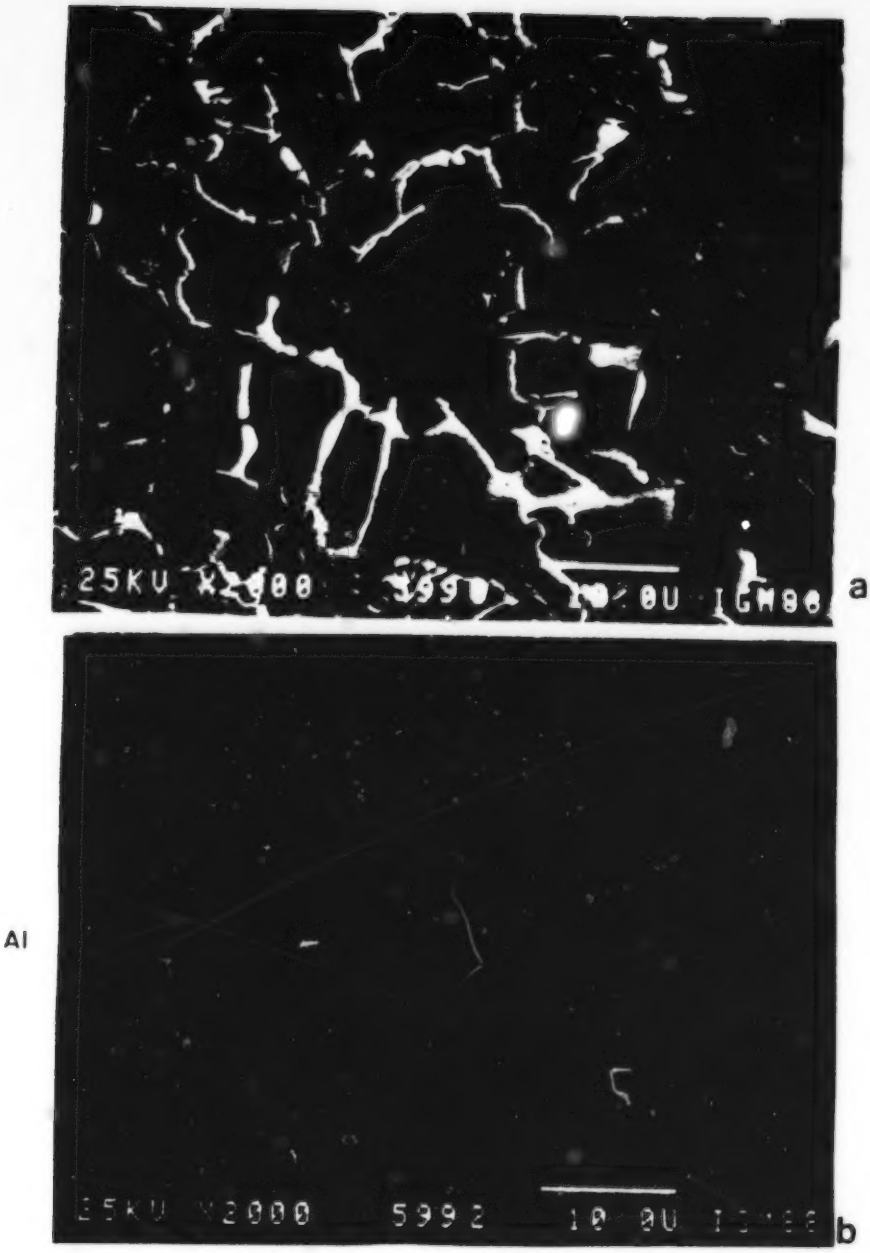

Fig. 8 a-b. SEM micrograph of the as-cast 380 alloy and the characteristic X-ray emission lines in SEM of Al, showing the eutectic constituants (Al-Si-Al_2Cu) and the α solid solution phase

Secondary dendrite arm spacing

A dendritic solidification structure is characteristic of all aluminum alloys casting. The mechanical properties of cast alloys are influenced by the dendrite arm spacing (Elliott, 1983; Bamberger and co-workers, 1987; Armstron and Jones, 1979; Oswald and Misra, 1981; Federick and Baily, 1968). The ultime tensile strength and elongation improve as the dendritic arm spacing is reduced. An increase in the solute content up to a eutectic composition leads to a decrease in the secondary dendrite arm spacing at a constant freezing rate (Bamberger and

co-workers, 1987; Young and Kirkwood, 1975). It is also well known that the secondary dendrite arm spacing (SDAS) decreases as the solidification time decreases. They are related by the following relationship (Fleming, 1984):

$$\lambda = A\, t_f^n \qquad (1)$$

where λ is the dendrite arm spacing (μm) t_f is the solidification time (s), and A and n are constants.

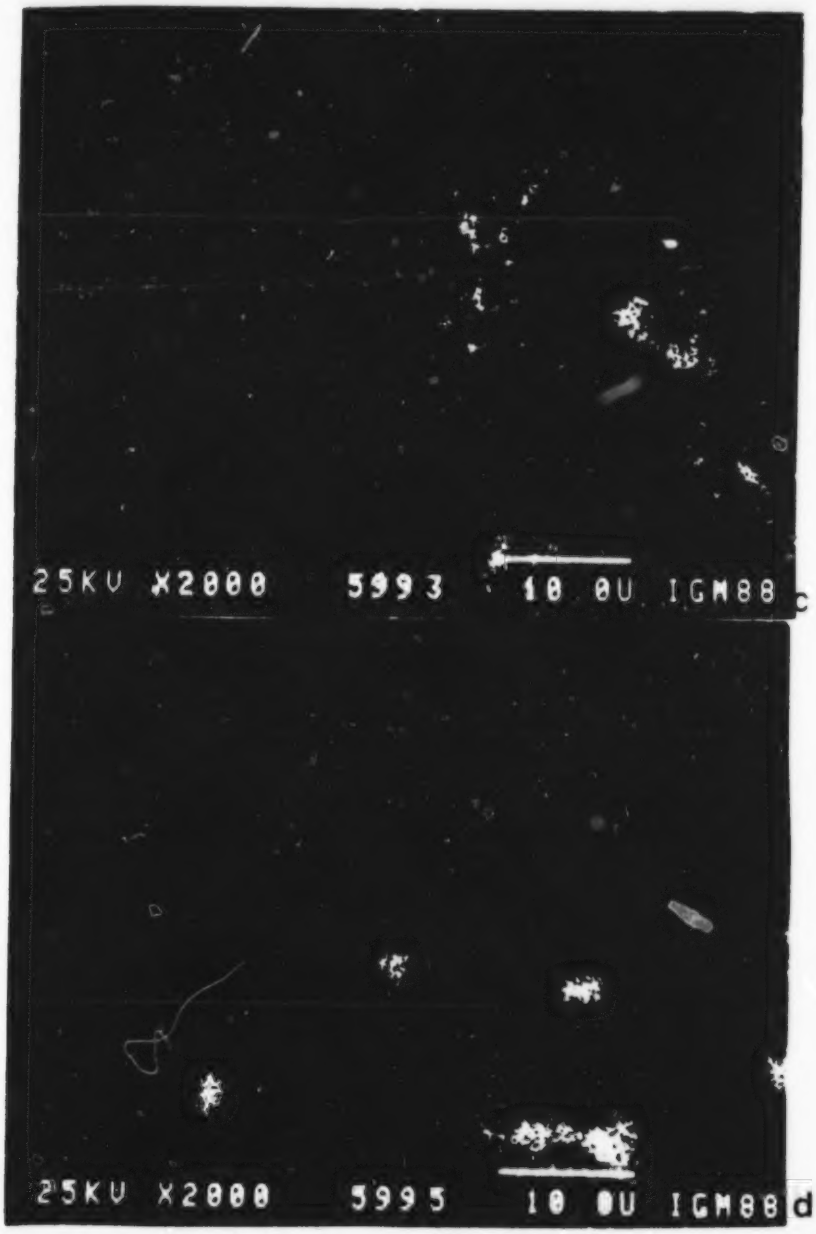

Fig. 8 c-d. SEM micrograph of the as-cast 380 alloy and the characteristic X-ray emission lines in SEM of Si and Cu, showing the eutectic constituants (Al-Si-Al_2Cu) and the α solid solution phase.

The dendrite arm spacing measurements in 380 alloy with respect to the distance from the wheel surface are illustratd in Fig. 9a. They increase with the above distance linearly on a logarithmic scale (Fig. 9b). Their relationship can, then, be expressed as follows:

$$\lambda = 5.3 \times {}^{0.13} \tag{2}$$

where x is the distance from the substrate in mm. The secondary dendrite arm spacing has varied from 3 to 6 μm.

Solidification model

Twin roll analysis. There is an increasing interest in the mathematical simulation of a wide range of processes involving solidification, such as strip casting process (Masounave and co-workers, 1988; Bagshaw and co-workers, 1986; O'Malley and Karabin, 1986; Kim and co-workers, 1986). The application of the enthalpy method to the phase change phenomenon was found relatively simple (Voller and Cross, 1981; Gutierrez and Szekely, 1986). It is useful to use one-dimensional model for the heat flow, particularly for high speed casting of thin strip (Jin and Sutherland, 1979; Clyne, 1984).

Assuming steady state conditions, the general partial differential equation describing the heat flow within the metal is:

$$V \frac{\partial H}{\partial x} = \frac{\partial}{\partial y} \left(K \frac{\partial T}{\partial y} \right) \tag{3}$$

where H, the enthalpy, may be expressed as:

$$H = \begin{cases} H_f + (T - T_L)\,\rho Cp + \rho Cp T_s & T \quad T_L \\ H_f \left(\dfrac{T - T_s}{T_L - T_s} \right) + \rho Cp\, T_s & T_s \quad T \quad T_L \\ \rho CpT & T \quad T_s \end{cases} \tag{4}$$

ρ is the density, Cp the specific heat, V the velocity of the strip, K the thermal conductivity and H_f the latent heat. In this model x is taken as positive in the casting direction and y as positive toward the slab centre. The melt is continuously supplied at a constant temperature To. The following simplifying assumptions were made:

- Conduction along the length of the strip is negligible in comparison with heat transfer in the y direction of the rolls.
- Conduction is negligible in the width direction, since the width of the strip is greater than its thickness.
- There is no slip between the strip and the rolls.
- Physical properties are temperature independant.

Using the following transformation:

$$x = Vt \tag{5}$$

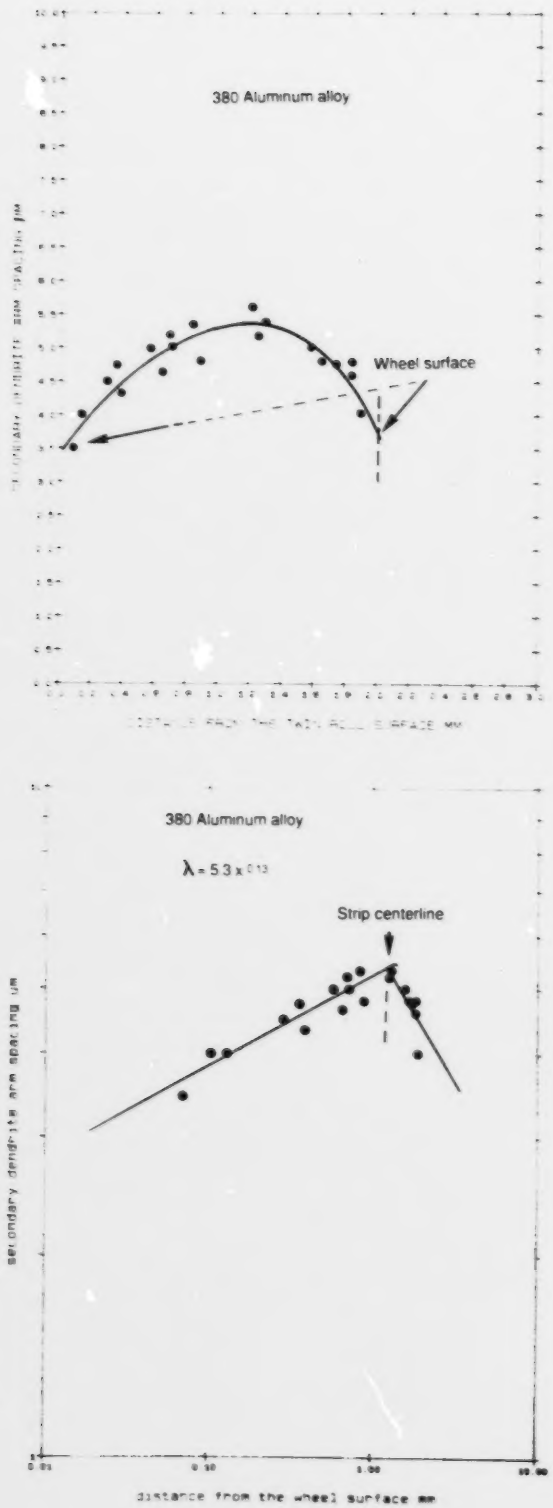

Fig. 9a-b. Dendrite arm spacing versus distance from one surface, on a linear and logarithmic scale respectively for the as-cast 380 alloy.

equation (3) becomes:

$$\frac{\partial H}{\partial t} = \frac{\partial}{\partial y}\left(K \frac{\partial T}{\partial y}\right) \tag{6}$$

where t is the residence time between the rolls taken for an element of volume of the strip. The above equation describes unsteady state, one-dimensional heat conduction of the imaginary element of thin strip moving with the same velocity V. It was solved by finite difference method using an implicit scheme.

The boundary conditions for heat transfert at the inlet, at the centre of the strip and at the roll/strip interface are given as follows:

- At the inlet the temperature of the liquid is constant and:

$$T = To \tag{7}$$

- At the centre line of the strip y = d/2 where d is its thickness:

$$q = - K \frac{\partial T}{\partial y} = 0 \tag{8}$$

- At the roll/strip interface:

$$q = h(T - Tw) \tag{9}$$

where h is the heat transfer coefficient and T the strip temperature at the interface and Tw the temperature of the roll.

Static mold analysis. Equation (6) can also describe the unsteady state heat flow in a static horizontal mold assuming that the thickness of the strip is smaller than its width. In this case the boundary conditions are as follows:

- Bottom surface of strip:

$$q = h\ (T - Tw) \tag{10}$$

- Top surface of strip:

$$q = hc\ (T - Ta) + \sigma \cdot \varepsilon \cdot (T^4 - Ta^3) \tag{11}$$

where hc is convection coefficient, σ is Stefan-Boltzmann constant, ε is emissivity and Ta is surrounding temperature.

RESULTS AND DISCUSSION

Static mold

The variation of temperature during solidification of 10 mm thick plates of the 1060 and 380 aluminum alloys is given in Fig. 10a and b (continuous line). The theoretical curves (dashed lines) are in good agreement with the experimental ones, using heat transfert coefficient values of 1.6 and 2 kW/m^2K respectively. These values are in accordance with data found in the literature in the range 1-2 $kW/m^2 \cdot K$ for aluminum in the static molds (Sully, 1976; Ho and Pehlke, 1983; Bamberger and co-workers, 1987).

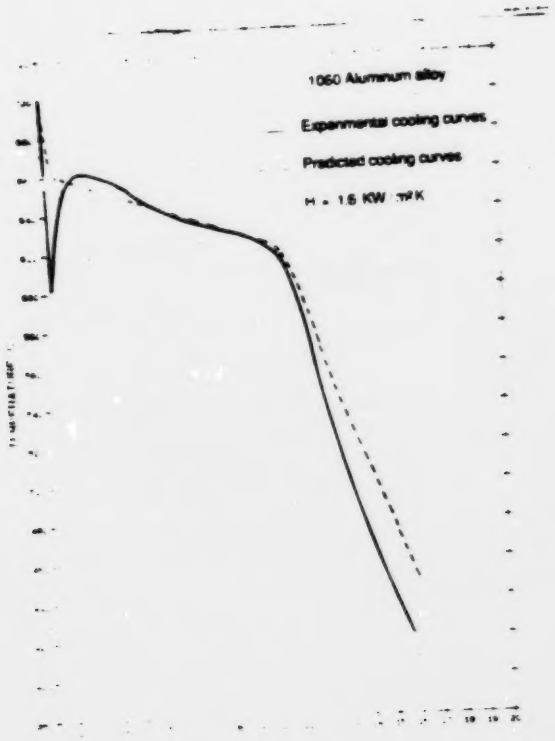

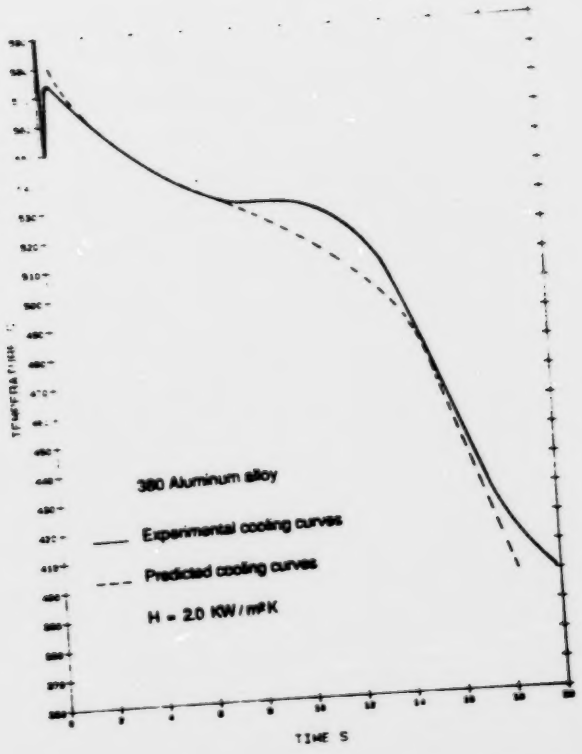

Fig. 10 a-b. Cooling curves of 1060 and 380 alloys respectively, cast on the horizontal static copper mold coated with grahite.

Strip casting of 380 alloy

The residence time of the strip of 380 alloy between the rolls during strip casting at 5 RPM is around 0.24 s. Using equation (5) the heat transfert coefficient that allows the strip to be completely solidified at the exit was found to be around 9 $kW/m^2 \cdot K$. The variation predicted by the model of the solidification time, t_f, with respect to the distance from the wheel, x, using the above value is given in Fig. 11. It indicates a linear relationship between the two parameters on logarithmic scale which can be expressed as follows:

$$t_f = 0.223\ x^{0.303} \tag{12}$$

expressing x with respect to t_f equation (2) becomes:

$$\lambda = 10.10\ t_f^{\ 0.43} \tag{13}$$

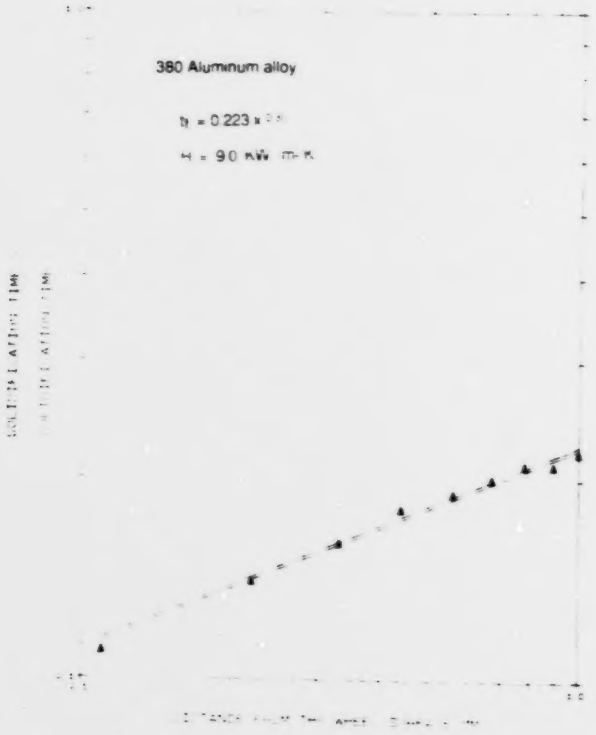

Fig. 11. Solidification time, t_f, with respect to the distance from the wheel surface to the centre of the strip.

The value of the exponent in equation (13) is in agreement with the value of 0.43 found by Bamberger and co-workers (1987) in the case of Al-Si alloys. It is also close to that of 0.39 published by Bower and co-workers (1976) for Al-Cu alloys, and that of 0.44 found for stainless steel (Steffen and Thielman, 1986). The constant 10.10 is lower than the value of 11.5 published by Bamberger and co-workers (1987) for Al-9.7% Si. As it was stated by the above authors, this constant is alloy dependant. It decreases as the alloying elements content

increases. Thus the lower value for alloy 380 can be expected since it contains the same amount of silicon but also has 3.3% Cu and 2.5% Zn.

CONCLUSIONS

The present investigation involved a study of the microstructure and segregation of strip cast 1060 and 380 aluminum alloy by a vertical twin roll caster. The following conclusions were reached:

1) The 1060 alloy during solidification, develops three zones: an undercooled structure (≈ 20 μm), a columnar zone and a cellular structure, with a solidification front boundary in the centre of the strip.

2) In the 380 alloy, a columnar dendritic structure of αAl solid solution is formed followed by an equiaxed dendritic zone. The interdendritic zone contains an eutectic of Al, Si and the intermetallic compound Al_2Cu with some microporosity along the centre line.

3) There is no macrosegregation but the microsegregation of Al, Si, Cu and Fe is greater in the central zone.

4) In 380 alloy the secondary dendrite arm spacing depends on the local solification time: $\lambda = 10.10\ t_f^{0.43}$. This relation can be used to determine the cooling rate related to the strip casting process.

5) The value of the heat transfer coefficient in the strip casting process was found to be 9. kW/m^2K. It is much higher than the value of 1.6 - 2. $kW/,m^2K$ in the static mold case.

Current work is now under way to cast aluminum and copper alloys strips on steel cylinders. Preliminary results show that strip reduction during casting enhances strip quality.

ACKNOWLEDGEMENT

The authors are indebted to Dr. D. Briggs and Dr. R. Thomson of CANMET for their assistance and discussion of this work. The authors would like to thank G. St-Amand, M. Thibodeau and J.-P. Nadeau for their technical help.

REFERENCES

Armstrong, G.R. and H. Jones (1979). Solidification and Casting of Metals, Metal Society, London, pp. 454-458.

Bagshaw, M.J., J.D. Hunt and R.M. Jordan (1986). Modelling and Control of Casting and Welding Processes. TMS/AIME, Warrendal, Pa., pp. 135-147.

Bamberger M., B.Z. Weiss and M.M. Stupel (1987). Met. Sci. and Tech., 3, pp. 49-56.

Blank, M., C. Caesar and U. Koster (1985). Rapidly Quenched Metals V., S. Steeb, and H. Warliment (Ed.), Amsterdam, p. 883.

Bower, T.F., H.D. Brody and M.C. Flemings (1976). Trans. AIME, 236, pp. 624-634.

Bowman, R.R. and S.D. Antolovich (1986). Metall. Trans. 17A, pp. 173-180.

Clyne, T.W. (1984). Metall. Trans., 15B, pp. 369-381.

Davies, G.J. and G.B. Brook (1983). Smithells Metals Reference Book, 6th Ed., Eric A. Brandes (Ed.), Chap. 10, p. 2.

Elliott, R. (1983). Eutectic Solidification Processing. Butterworths Ed., pp. 182-188.

Fleming, M.C. (1984). Solidification Processing, McGraw-Hill, New York, pp. 146-150.

Frederick, S.F. and W.A. Baily (1968). Trans. Metall. Soc., AIME, 242, p. 2063.

Grugel, R. and W. Kurz (1987). Metall. Trans., 18A, pp. 1137-1142.

Gutierrez, E.M. and J. Szekely (1986). Metall. Trans., 17B, pp. 695-703.

Ho, K. and R.K. Pehlke (1985). Metall. Trans., 16B, pp. 585-594.

Jin, I. and J.G. Sutherland (1979). Solidification and Casting of Metals, Metal Society, London, pp. 256-259.

Kim, Y.G., B. Farouk and J. Keverian (1986). Manufacturing Simulation and Processes, 20, ASME, pp. 277-288.

Masounave, J., J. Blain and E. Essadiqi (1988). Séminaire sur les nouvelles applications de l'acier face à la concurrence des matériaux de substitution, Commission Économique pour l'Europe, Luxembourg, 2 au 6 mai.

McCall J.L. (1979). Properties and Selection - Non Ferrous Alloys and Pure Metals, Metals Handbook, 9th Ed. ASM, Metals Park, Ohio 44073, p. 64.

McCall J.L. (1979). Properties and Selection - Non Ferrous Alloys and Pure Metals, Metals Handbook, 9th Ed. ASM, Metals Park, Ohio 44073, p. 170.

Morris, M.A. and D.G. Morris (1987). Acta Metall. 35, pp. 2511-2522.

O'Malley, R.J. and M.E. Karabiu (1986). Modelling and Control of Casting and Welding Processes. TMS/AIME, Warrendal, Pa., pp. 149-168.

Oswald K.J. and M.S. Misra (1981). AFS International, Cast-Metal J., 6, p. 23.

Steffen, R. and R. Thielmann (1986). Stahl u Eisen, 106, pp. 631-640.

Sully, L.J.D. (1976). Trans AFS, 84, pp. 735-744.

Voller, V. and M. Cross (1981). Int. J. Heat Mass Transfer, 24, pp. 545-556.

Young, K.P. and D.H. Kirkwood (1975). Metall. Trans. 6A, pp. 197-205.